

On the experimental calculation of the conversion matrix for sub-harmonic mixer

G. Loglio, A. Cidronali, C. Accillaro, M. Usai, I. Magrini, M. Camprini, G. Collodi, G. Manes

Dept. Electronics and Telecommunications University of Florence, Florence 50139 Italy;
loglio@ing.unifi.it; fax: +39.055.494569 ; tel: +39.055.4796369

Abstract — This paper introduces experimental observations and theoretical considerations on a newly introduced technique allowing to measure the admittance conversion matrix of microwave device, by large-signal vectorial measurements. In particular, it discusses the capability and the limitation of the method to evaluate the conversion matrix of an anti-parallel Schottky diode-pair, starting from the measurement of the single diode. A theoretical treatment and several simulated and experimental results give an insight into the approach.

I. INTRODUCTION

Nonlinear vectorial network analyzers (N VNAs) have been used to characterize and model nonlinear microwave devices and circuits [1-4]. Recently a technique to extract the conversion matrix starting from the vectorial large-signal measurement has been proposed, [7-8], as a step toward the direct inclusion of the results deriving from vectorial large signal characterization, in the synthesis protocol of microwave mixer. The paper purpose is to discuss the possible extension of this method to derive the conversion matrix of a nonlinear cell starting from vectorial large signal measurement of a cell's sub-set. In particular we discuss the possibility to calculate the conversion matrix of an anti-parallel Schottky diode-pair starting from the measurement of that of the single diode. The motivation of the work doesn't consist in the reduction of the measurement complexity but, rather, the discussion of the extension of the proposed method to completely new device configuration of practical interest. In the paper it is shown that, although in certain selected cases it is theoretically possible, the non-idealities and the presence of significant junction capacitance permit only an approximation of the searched conversion matrix.

The paper is organized as follows. The characterization method is described with reference to the particular topology of the nonlinear cell under consideration. Then, a number of simulated and measured experimental results are discussed in detail, describing the potentials and limitations of this approach for mixer design.

II. ANALYTICAL DISCUSSION

Let us recall the basics of the extraction of the conversion matrix method for what concerns the specific interest of the calculation of anti-parallel diodes.

In the extraction methods [7-8] the relationships relating the current and voltage phasors at intermodulation products are linear, and they are ruled by the conversion matrix:

$$\mathbf{I} = [\mathbf{Y}] \cdot \mathbf{V}$$

The symbol $[\mathbf{Y}]$ represents the conversion matrix, which is, in fact, a linearization of the DUT, under the large-signal state, with respect to the small signals. The local oscillator pump takes part of the linearized system, so that the matrix $[\mathbf{Y}]$ will depend on the pump voltage excitation – magnitude and chosen reference phase ϕ_0 .

As a straightforward consequence of that, selecting different values for ϕ_0 is equivalent to drive the device with different LO phases. This feature exhibits a practical application in case two diodes are driven respectively with $\phi_0 = 0$ and $\phi_0 = \pi$; consequently it may be possible to derive the conversion matrix for a single diode selecting $\phi_0 = 0$, then re-use the same measurement selecting $\phi_0 = \pi$, and adding the two matrices to obtain the conversion matrix of the pair.

This has important additional constraints to be effectively applied. The first is that the single and the pair case must have the same the same derivative of the current with respect to the LO signal. This condition is analyzed in detail in the following.

Let us consider the simplest diode model:

$$I(V) = \begin{cases} 0 & \text{where } V < 0 \\ f(V) & \text{elsewhere} \end{cases}$$

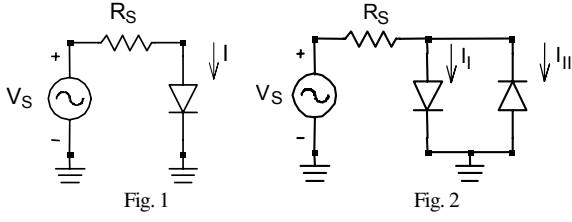
and perform a large-signal small-signal analysis to the simple circuit in Fig. 1, we obtain a time-varying conductance [5-6]:

$$g(t) = \begin{cases} \left. \frac{d}{dV} f(V) \right|_{V=V(t)} & \text{if } t \in [0, T/2] \\ 0 & \text{if } t \in [T/2, T] \end{cases}$$

where

$$\begin{aligned} V(t) &= V_s(t) - I(V(t)) \cdot R_s = \\ &= \begin{cases} V_s(t) - f(V(t)) \cdot R_s & \text{if } t \in [0, T/2] \\ V_s(t) & \text{if } t \in [T/2, T] \end{cases} \end{aligned}$$

We focus on the arising implications, when connecting in anti-parallel pair two identical devices having that particular $I(V)$ characteristic. Fig. 2 reports the arrangement which is a very common topology in sub-harmonically pumped mixer applications.



In general, it is not possible to derive the conversion matrix of a diode pair starting from the measured conversion matrix of a single diode, due to different large-signal excitation. However, assuming the property we stated is true, we now demonstrate that large-signal excitation deviations do not theoretically affect the time-varying conductance and therefore the conversion matrices.

Indeed, significant variations exist in the voltage waveform, between this circuit and the previous one. In fact, in both half-periods a non-zero current flow causes a voltage drop across the source resistance, giving rise to a symmetrical shape, therefore annealing every even-order harmonics and globally changing the spectral composition of the large-signal excitation.

On the other hand, such variations appear only in the half-period in which each diode is brought in interdiction. So, in each branch of the pair, both the instantaneous large-signal current and the time-varying conductance assume the same values as in the single-diode case. With reference to Fig. 2, it is possible to write:

$$I_i(t) = \begin{cases} f(V(t)) & \text{if } t \in [0, T/2] \\ 0 & \text{if } t \in [T/2, T] \end{cases}$$

$$I_{ii}(t) = \begin{cases} 0 & \text{if } t \in [0, T/2] \\ -f(-V(t)) & \text{if } t \in [T/2, T] \end{cases}$$

$$g_i(t) = \begin{cases} \left. \frac{d}{dV} f(V) \right|_{V=V(t)} & \text{if } t \in [0, T/2] \\ 0 & \text{if } t \in [T/2, T] \end{cases}$$

$$g_{ii}(t) = \begin{cases} 0 & \text{if } t \in [0, T/2] \\ \left. -\frac{d}{d(-V)} f(-V) \right|_{V=V(t)} & \text{if } t \in [T/2, T] \end{cases}$$

where

$$V(t) = V_s(t) - I(V(t)) \cdot R_s = \begin{cases} V_s(t) - f(V(t)) \cdot R_s & \text{if } t \in [0, T/2] \\ V_s(t) + f(-V(t)) \cdot R_s & \text{if } t \in [T/2, T] \end{cases}$$

Notice that in each current and conductance assignment the large-signal excitation is exactly the same as in the single-diode case, if we restrict to the conducting half-period. At this point, it should be clear that the conversion matrix of the diode pair can be found by simply adding the conversion matrix extracted for a single diode to that extracted for the same diode, but with a $T/2$ shift in the time-reference system:

$$g_{i+ii}(t) = g_i(t) + g_{ii}(t) = g(t) + g(t+T/2)$$

III. EXPERIMENTAL RESULTS

The method explained in Section II is applied to measuring the conversion matrix of commercially available diodes manufactured by HP, part number HSMS8202. This part includes two general-purpose Schottky diodes, packaged in the same die, connected in series with access to the central knot.

First, the method is simulated on ideal devices satisfying the theoretical requirements evidenced in the previous section. They are represented by a static nonlinear voltage-controlled current source, whose analytical expression is obtained from a polynomial fitting of DC measurements of the diodes in our case study; no dynamic behaviour is included in such a model. In this way, no current flows during the negative half-wave of the driving voltage.

A virtual measurement bench is set up on an Harmonic Balance simulator, injecting the combination of a large signal ($f_{LO} = 2.6\text{GHz}$, power ranging from -5 to $+10$ dBm) and a small tone ($f_n = n f_{LO} \pm f_{IF}$, with $f_{IF} = 650\text{MHz}$, -40 dBm power), giving an output that is qualitatively homogeneous with NVNA measurements required by the method in [7-8] to extract Conversion Matrices (CMs). Several CMs are extracted, for different numbers of considered harmonics.

Now, let us focus on an outstanding property of the method, i. e. the arbitrary choice of the fundamental pump-voltage initial phase ϕ_b . By performing distinct extractions with $\phi_b = 0$ and $\phi_b = \pi$, we obtain two conversion matrices Y_0 and Y_π for the same device, with a difference in the time-reference shift only. They can be associated to the time-domain conductances of forward and reverse diode, respectively. As a straightforward consequence of Section II, $Y_{PAIR} \cong Y_0 + Y_\pi$ where the conversion matrix of the anti-parallel pair Y_{PAIR} is not perfectly equal to the right-hand term, because of limitations in accuracy due to the truncation of the otherwise indefinitely extended matrices. Then, comparisons are displayed between CMs obtained by this kind of calculation and CMs directly extracted from the simulation of a network in which two such ideal devices have been connected in anti-parallel. In particular, Fig. 3 reports the relative error between the parameter $Y_{2,0}$ obtained in the two different ways; notice that $Y_{2,0}$ is the most significant parameter for the conversion in a sub-harmonically pumped mixer, since it represents the transadmittance from the input voltage and the converted current.

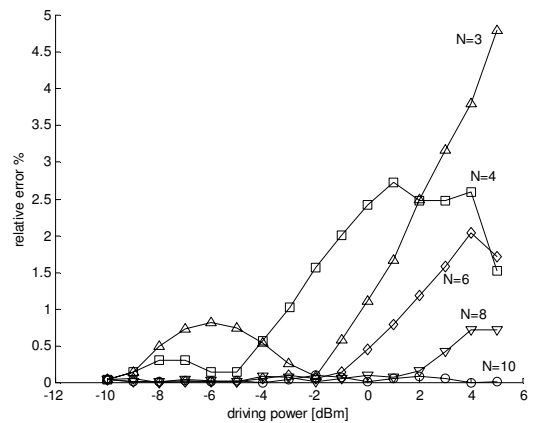


Fig. 3. Relative error of $Y_{2,0}$ parameter of CMs at different driving powers, truncated to $N=3$ (triangles), $N=4$ (squares), $N=6$ (diamonds), $N=8$ (reverse triangles) and $N=10$ (circles) considered harmonics.

Subsequently, a parallel capacitor is added to the simulated networks, in order to study the influence of the junction capacitance unavoidably there in real devices. Results are collected for growing values of the capacitance, evidencing in Fig. 4 the effect of gradually violating the hypothesis which requires a null current during the negative half-wave of the driving voltage.

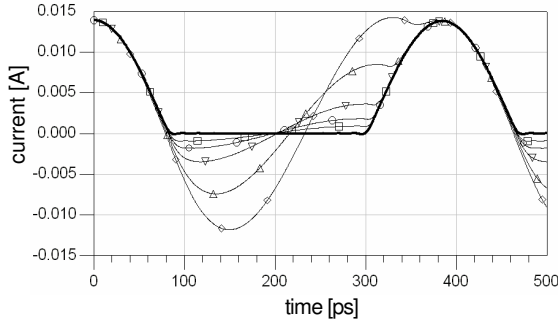


Fig. 4. Time-domain current waveforms at the maximum driving power, on an ideal diode with junction capacitances of 50fF (squares), 100fF (circles), 200fF (reverse triangles), 500fF (triangles) and 1pF (diamonds). Thick curve is without capacitor.

As a consequence, CMs extracted from these simulations, and treated as explained above, differ from those directly obtained by the device pair, even though they are truncated at a large number of considered harmonics, namely $N = 10$. Fig. 5 displays the comparison, giving an estimate of the relative error that can be expected because of this kind of non-ideality.

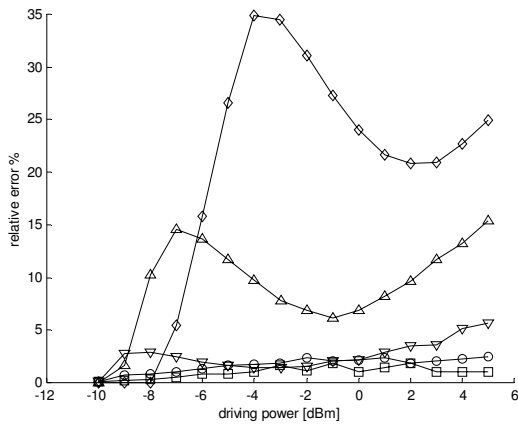


Fig. 5. Relative error of $Y_{2,0}$ parameter of CMs at different driving powers, considering devices with junction capacitances of 50fF (squares), 100fF (circles), 200fF (reverse triangles), 500fF (triangles) and 1pF (diamonds).

Finally, real devices are measured.

The used NVNA consists of a 4-channel data acquisition system and provides magnitude and phase values of the incident and scattered complex wave variables at both ports of the device on a user-defined grid. In particular the complete set-up in our case consisted of two RF sources, four directional couplers, an RF to IF down converter and a data acquisition system. The two RF sources can be combined to supply the desired excitations at port 1 or port 2, but in this experiment only port 1 was excited. An appropriate amplitude and phase calibration procedure allows the correction of the “raw” quantities. The set-up is shown in Fig. 6, where a large signal is applied to the DUT’s port 1

and it is combined with a second signal, namely a small level signal; the second port is left open. The NVNA is able to measure both the harmonics of the large signal and the mixing products, if the calibration grid contains the frequencies of interest.

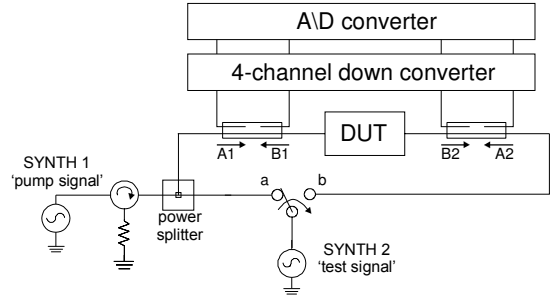


Fig.6 Set-up adopted for the conversion matrix extraction, based on NVNA (switch is always in position “a”).

The admittance conversion matrix of a single diode is extracted, and metal pads and transmission lines (necessary to access the device) are de-embedded. The number of considered harmonics is set to $N = 4$, which is consistent with the instrumentation bandwidth. Several matrices are collected at growing pump power levels, ranging from around -10 to +5 dBm, similar as in above-mentioned simulations.

What could be expected, reverse current flows, due to junction capacitances, as shown in time-domain current waveform in Fig. 7.

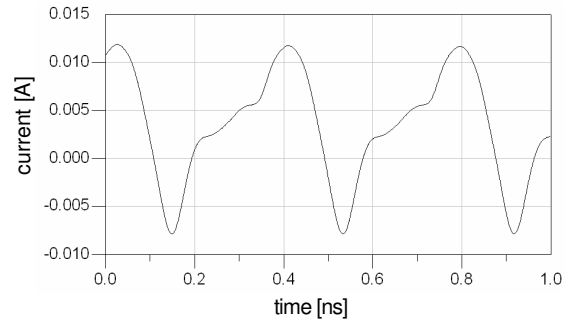


Fig. 7. Time-domain current waveforms at the maximum driving power, on a real diode. Notice the effect of charge-storage and discharge with consequent reverse conduction.

In order to complete the comparison, another extraction is performed, by measuring a diode pair physically connected in anti-parallel. Measurement conditions are kept similar to those in the previous case. In spite of non-ideal characteristics of real devices, derived and directly-extracted conversion matrices show similarities with an accuracy comparable to the expected one. Fig. 8 reports the relative error between the parameter $Y_{2,0}$ calculated from single-diode measurements as in Section II and the one directly obtained from diode-pair measurements. Magnitudes of such parameter are plotted as functions of driving power, as well, in Fig. 9.

Regarding previous simulations, it can be stated that the error due to truncation for $N = 4$ is around 3%, while a junction capacitance giving similar current waveform bring to around 16% error. Therefore, by simply assuming that errors due to different error-sources can be added together, we could expect a combined error of around 19%. Even though the relative error slightly exceed this value, results can be considered satisfactory, since parasitics, measurement errors,

and other elements contributing to the overall difference were not taken into account in this quantitative comparison.

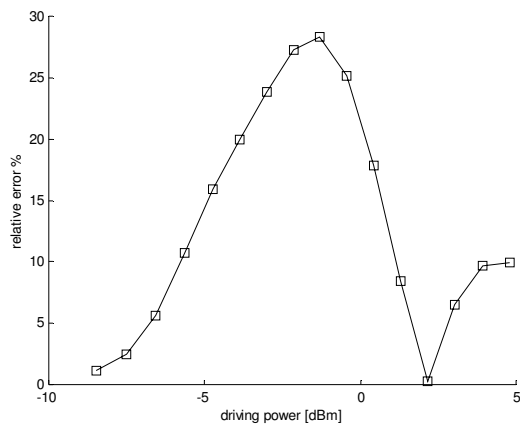


Fig. 8. Relative error of Y_{20} parameter of CMs at different driving powers, for measured real devices.

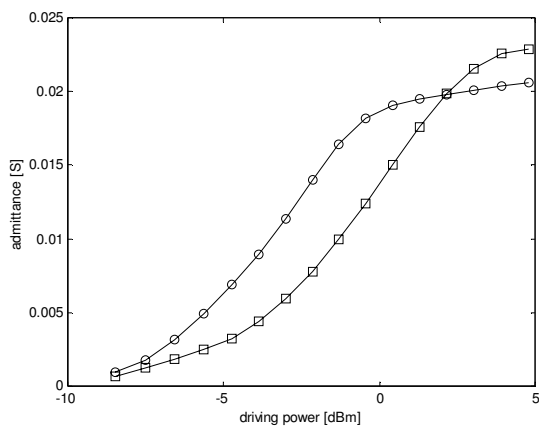


Fig. 9. Magnitude of Y_{20} parameter of derived (circles) and directly-measured (squares) CMs at different driving powers, for measured real devices.

If we represent the matrices so that the magnitudes of their elements are logarithmically related to grey tones, we can see a qualitative agreement, especially in the rejection of even-order intermodulation products, which are related to side-diagonal terms in the CMs (Fig. 10-11). This is expected for the odd-characteristic of an anti-parallel diode-pair.

IV. CONCLUSION

This paper had dealt with the possibility to extract the conversion matrix of an anti-parallel Schottky diode pair, starting from the measurement of the single diode. The approach refers to a previously proposed method which allow to measure the admittance conversion matrix of microwave devices, by means of large-signal vectorial measurements.

The theoretical treatment has shown that it was in principle possible; however, non-idealities make the approach effective only on a qualitative way. The experimental results presented here made use of a prototype based on commercially available SMD diodes, and considered the frequencies $LO/RF/IF = 2.6\text{GHz}/5.85\text{GHz}/650\text{MHz}$. The discussion on this results is intended to stimulate further debate on this topic.

ACKNOWLEDGEMENT

Research reported here was performed in the context of the network TARGET – “Top Amplifier Research Groups in a European Team” and supported by the

information Society Technologies Programme of the EU under contract IST-1-507893-NOE, www.target-org.net.

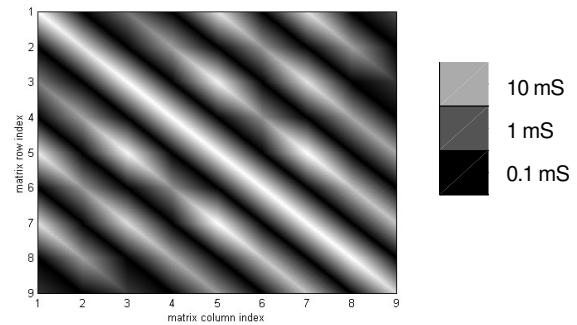


Fig. 10. Grey-tone representation of the CM of a diode-pair calculated by means of single-diode measurements

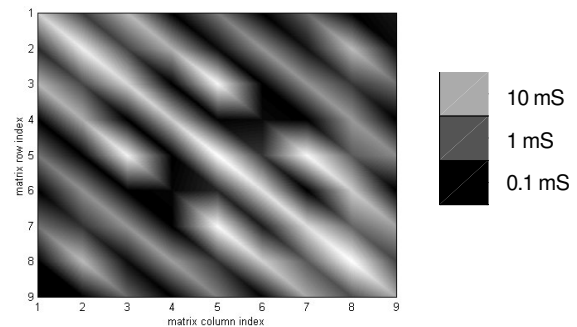


Fig. 11. Grey-tone representation of the CM of a diode-pair directly extracted by two-diode measurements

REFERENCES

- [1] D. Barataud et al., “Measurement and Control of Current/Voltage Waveforms of Microwave Transistors Using a Harmonic Load-Pull System for the Optimum Design of High Efficiency Power Amplifiers,” *IEEE Trans. on Instrumentation and Measurement*, Vol. 48, No. 4, pp. 835-842, August 1999.
- [2] J. Verspecht and P. Van Esch, “Accurately characterizing of hard nonlinear behaviour of microwave components by the Nonlinear Network Measurement System: introducing the nonlinear scattering function”, *Proc. International Workshop on Integrated Nonlinear Microwave and Millimeterwave Circuits*, (Duisburg, Germany), 10-11 October, 1996, pp. 17-26, Duisburg, October 1998.
- [3] J. A. Jargon, K. C. Gupta, D. Schreurs, and D. C. DeGroot, “Developing Frequency-Domain Models for Nonlinear Circuits Based on Large-Signal Measurements,” *Proc. of the 27th General Assembly of the Intern. Union of Radio Science*, CD-ROM A1.O.6, Maastricht, the Netherlands, Aug. 2002.
- [4] D. Schreurs et al, “Direct extraction of the non-linear model for two-port devices from vectorial non-linear network analyzer measurements,” *European Microwave Conf.*, pp. 921-926, 1997.
- [5] H.C. Torrey and C.A. Whitmer, “Crystal Rectifiers,” New York: McGraw-Hill, 1948.
- [6] S.A. Maas, “Nonlinear Microwave Circuits,” Piscataway, N.J.: IEEE Press, 1997.
- [7] A. Cidronali, K.C. Gupta, J. Jargon, K.A. Remley, D. DeGroot, G. Manes, “Extraction of Conversion Matrices for P-HEMTs based on Vectorial Large Signal Measurements”, *International Microwave Symposium Digest*, Philadelphia, USA, June 2003.
- [8] A. Cidronali, G. Loglio, J. Jargon, K.A. Remley, I. Magrini, D. DeGroot, D. Schreurs, K.C. Gupta, G. Manes, “RF and IF mixer optimum matching impedances extracted by large-signal vectorial measurements,” *European Gallium Arsenide and related III-V Compounds Application Symposium (GAAS) 2003*, pp. 61-64, Munich, 6-10 October 2003.